# WAVELET BASED STATOR INTER-TURN FAULTS DETECTION IN THREE-PHASE INDUCTION MOTORS OPERATED UNDER NOISY CONDITION

**N. Rama Devi***
Associate Professor, Department of EEE
Bapatla Engineering College, Bapatla, India
Email: ramadevi_eee@yahoo.co.in

**D.V.S.S.Siva Sarma**
Professor, Department of EEE
NITW, Warangal, India
Email: sivasarma@ieee.org

**P.V.Ramana Rao**
Professor, Department of EEE
ANU college of Engineering, Guntur, India
Email:pvr_eee@yahoo.co.in

***Abstract:*** *The motor current signature analysis is widely used for diagnosis of various industrial motor faults. Generally, the captured current signals are corrupted by noise. In order to extract the fault feature from noisy current signals, the corrupted current signal has to be preprocessed by some means. This paper proposes a wavelet and adaptive threshold based approach to detect and identify stator inter-turn faults in three-phase induction motor. A stationary wavelet transform is used to find the fault residue present in the three-phase stator currents. These three-phase residue currents are again decomposed with discrete wavelet transform to extract the disturbance. Fault index and three-phase energies are defined and compared with adaptive thresholds to detect the transients and its location. The sensitivity of stator inter-turn fault to the number of shortened turns is also analysed. Finally, the algorithm is tested with both simulation as well as practical data for various levels of stator inter-turn faults. The validity and effectiveness of the proposed algorithm is clearly shown from obtained results.*

***Keywords:*** *Fault index, Induction motor, Residue currents, stator inter-turn fault, stationary wavelet transform*

## 1. Introduction

ELECTRIC motors are essential components of many industrial processes. Squirrel cage induction motors are more prevalent in use than other motors due to their ruggedness, low cost and maintenance and ease of operation. Generally, motors undergo various stresses during their operation and these stresses might lead to several failures. Hence condition monitoring becomes crucial for induction motors in order to avoid disastrous failures [1]. Several studies have reported that 30-40% of induction motor failures are due to stator winding insulation breakdown (e.g. turn-turn, line to ground and line to line faults) [2]. The stator internal faults start with turn-turn short circuit; the undetected turn-to-turn winding faults finally grow and culminate in major faults such as phase to ground and phase to phase faults. Therefore, early detection of stator inter-turn fault eliminates subsequent damage to the motor [3], thereby reducing repair cost and motor down time.

Various online and offline monitoring techniques and their relative merits are summarized in [4]. The feasibility of the existing monitoring methods for medium voltage induction motors is presented in [5]. A large amount of research has been directed towards the electrical monitoring of motor current signature analysis (MCSA), which is recognized as a standard for monitoring of motor faults due to its simplicity. The main advantage of MCSA is to analyze the stator current in search of current harmonics directly related to new rotating flux components, which are caused by faults in the motor-flux distribution. Detection of faults using $dq0$ components [6] and the envelope of the stator currents [7]are fundamentally same as the current component method. Observer-based method is proposed [8] to detect the stator inter-turn faults, but this approach suffers from model accuracy. The detection of stator inter-turn fault using Fourier transform is discussed in [9] and [10]. Generally, Fourier analysis that is applicable for stationary signals can not be applicable for non-stationary signals. This limitation can be overcome by using time-frequency analysis. Wavelet transform is a powerful tool for condition monitoring and fault diagnosis in induction motor [11], [12].

In harsh industrial environments the noise level and its variation should be considered precisely for fault diagnosis because the fault signature due to stator inter-turn short circuit is much lower than the noise level. Hence, it requires a good

*Author correspondence, ramadevi_eee@yahoo.co.in

technique with a capability to suppress the noise without corrupting the fault signature. The discrete wavelet transform (DWT) is not suitable for signal noise reduction applications due to the lack of invariant translation property. But this effect can be overcome using stationary wavelet transform (SWT) that has been discussed in [13] and [14]. Most of the existing techniques require some sort of domain expertise to identify whether the three-phase induction motor is operating in normal or abnormal condition. In actual practice, the captured currents are influenced by many factors, which includes supply unbalance, static eccentricity and noise. These conditions may lead to errors in fault detection. Hence, an accurate inter-turn fault diagnosis techniques must be required to detect the inception of a fault, its location and severity.

This paper proposes an algorithm, to detect and identify stator inter-turn faults in three-phase induction motor, based on wavelet transform and adaptive thresholds. The three-phase stator currents are captured with a sampling frequency of 6.6KHz. The three-phase residues are obtained by analysing the three-phase stator currents with SWT of Biorthgonal 5.5 (Bior5.5) mother wavelet upto $6^{th}$ level. These residues are again decomposed with DWT of same mother wavelet to predict the fault. The detection and identification of the fault is performed by using defined fault index and three-phase energies. The proposed algorithm is tested for fault detection and identification from three-phase currents obtained in simulation as well as the experimental setup. The proposed adaptive threshold based algorithm improves the fault detection and identification accuracy.

## 2. Stationary Wavelet Transform

The SWT is similar to the DWT but it does not use down-sampling. In SWT, the downsampling stage at each scale of DWT is replaced by an upsample of the filter before the convolution. Suppose we are given a signal $x(n)$ of length N where N =$2^J$ for some integer J. Let $h_1(n)$ and $g_1(n)$ be the impulse responses of the high-pass filter and the low-pass filter. The impulse responses are chosen such that the outputs of the filters are orthogonal to each other. At the first level of SWT, the input signal $x(n)$ is convolved with $h_1(n)$ to obtain the detail coefficients $d_1(n)$ and with $g_1(n)$ to obtain the approximation coefficients $a_1(n)$, i.e

$$d_1(n) = h_1(n) * x(n) = \sum h_1(n-k)x(k) \tag{1}$$

$$a_1(n) = g_1(n) * x(n) = \sum g_1(n-k)x(k) \tag{2}$$

The length of $a_1(n)$ and $d_1(n)$ are N instead of N/2 as in the DWT case because no sub-sampling is performed. At the next level of the SWT, $a_1(n)$ is used to generate $d_2(n)$ and $a_2(n)$ with modified filter $h_2(n)$ and $g_2(n)$, which are obtained by up sampling $h_1(n)$ and $g_1(n)$ respectively.

$$d_2(n) = h_2(n) * a_1(n) = \sum h_2(n-k)a_1(k) \tag{3}$$

$$a_2(n) = g_2(n) * a_1(n) = \sum g_2(n-k)a_1(k) \tag{4}$$

This process is continued recursively. Compare with the traditional wavelet transform, the SWT has several advantages which are reported in [15]. In wavelet analysis, the threshold selection plays a key role in noise elimination process. In [16] various threshold schemes are introduced and discussed in a general context. Though, Universal threshold (fixed threshold) selection rule is the most widely used, the variance of the noise signal changes with time is a practical limitation with this scheme. Hence, interval or level based threshold selection is preferable. In general, selection of mother wavelet is based on the type of application. In the proposed algorithm, Bior5.5 wavelet has been used as the wavelet basis function for fault detection and identification.

## 3. Fault Detection and Identification Algorithm

The proposed fault detection algorithm starts with data acquisition and then application of wavelet analysis and adaptive threshold logics. This is illustrated in Fig. 1. The threshold based reconstruction of the three-phase stator currents should compensate the effects due to supply unbalance and machine unbalance. The residues of three-phase stator currents were obtained by using stationary wavelet denoising technique of level based threshold. The three-phase currents of the motor are decomposed with SWT of Bior5.5 to obtain approximate and detail level coefficients upto $6^{th}$ level. The thresholds of $d1$ coefficients to $d4$ coefficients are made maximum while threshold value of $d5$ coefficients is set to a high value as this band of frequency components is sensitive to the supply unbalances. The threshold value of $d6$ is calculated based on its peak value in 1st cycle and multiplied with a distortion factor which is calculated from RMS value of the current signal during start-up (preferably in $1^{st}$ cycle). The threshold value of d6 coefficient may enhance the fault signature, because the pre-fault value is subtracted from the captured signal. Therefore, the reconstructed signals are called as fault residues. The residue of three-phase stator currents are again decomposed with a DWT of Bior5.5 and the slopes of each phase detail ($d1$) coefficients are calculated for identifying the variation levels due to disturbances. The sum of absolute slope of the detailed level coefficients is set as a fault index ($I_f$) and it is described mathematically as follows.

$$I_f(n) = |slope\_d1I_R(n)| + |slope\_d1I_Y(n)| + |slope\_d1I_B(n)| \tag{5}$$

where $n = 1 : N_1$; $N_1$ is Total samples; $slope\_d1I_R$, $slope\_d1I_Y$, and $slope\_d1I_B$ are the slopes of d1 coefficients of residue currents in R, Y and B phases respectively. The abnormal condition of the induction motor can be identified by checking three consecutive fault indices values with an adaptive threshold $Th1$ and count value of these fault indices over a window of 10 samples should be greater than 6. The disturbance corresponding instant is calculated from the 1st

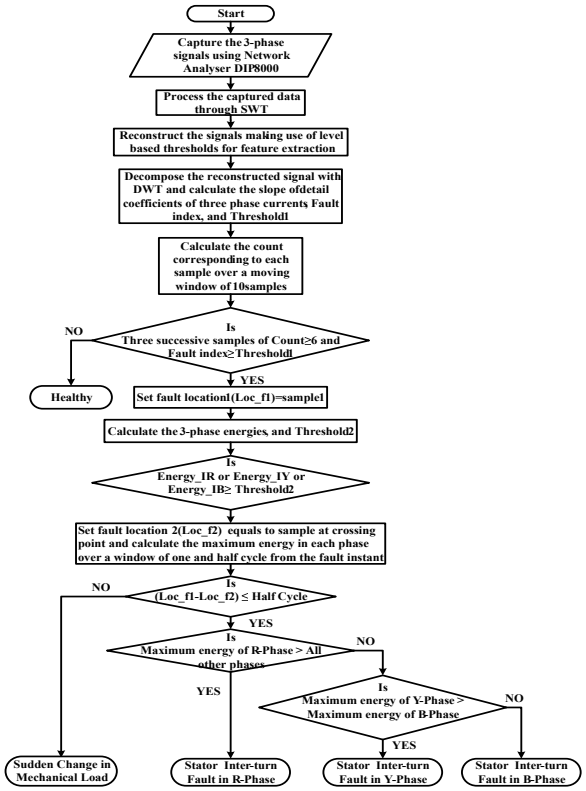


Fig. 1. Flow chart for stator inter-turn fault detection and identification

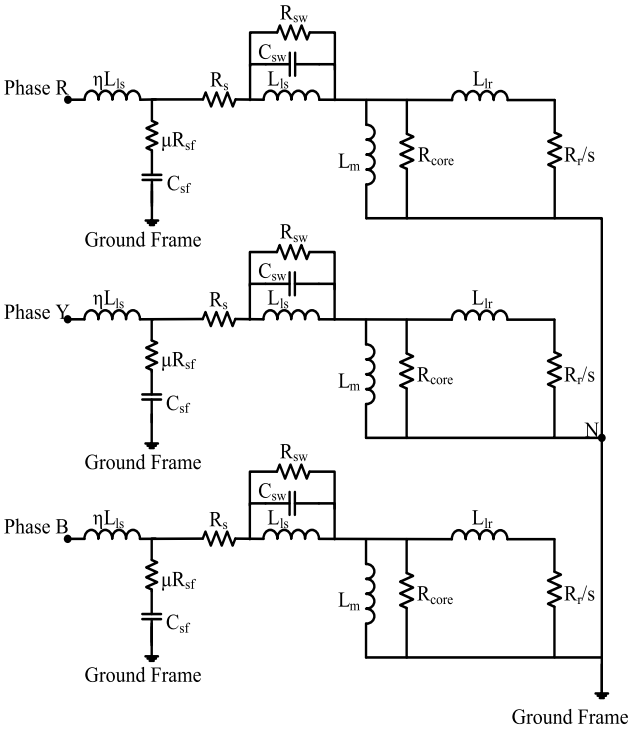


Fig. 2. Three-phase induction motor model.

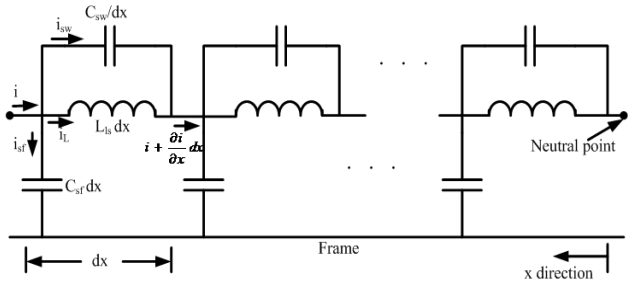


Fig. 3. Distributed high frequency model for stator winding

sample of the three consecutive fault indices and it is defined as location one ($Loc1$). The type of disturbance present in the system is obtained by using three-phase energy values, which are compared with adaptive threshold $Th2$. The energy crossing point with respect to adaptive threshold $Th2$ is defined as location two ($Loc2$). The adaptive $Th1$ and adaptive threshold $Th2$ are calculated based on fault index statics and three-phase energy statics respectively. The three-phase energies are defined mathematically as follows.

$$Energy\_I_j(n) = \frac{1}{N_2}\sum_{m=1}^{N_2} slope\_d1I_j(m)^2 \qquad (6)$$

where $j \in R,Y,B$ and $N_2$ is quarter cycle samples

A sudden mechanical load change may also lead to transients in stator currents. But, it should be discriminated from the stator inter-turn faults by using fundamental concept of time constant representing mechanical and electrical systems. Hence, the stator inter-turn faults and sudden change in mechanical load should be discriminated by taking the difference between the disturbance instants, which are obtained from energy and fault index. The faulty phase of the stator inter-turn fault is identified by comparing the maximum energy obtained in each phase over one and half cycle from fault instant.

## 4. Distributed Parameter Model and Validation

Machine modeling under fault conditions is a key factor for predicting its behaviour. The availability of more powerful computers and the development of new machine models are able to manage geometry together with electric and magnetic features. This allows to move from the earlier models of faulty machines referred as steady-state operations to sophisticated models of transient operation. Induction motor is subjected to switching transients and its effects can be analysed with the help of high frequency model only. Figure 2 represents the universal model of a three-phase induction motor. Each coil of the stator winding is represented by a distributed $\pi$ model as shown in Fig. 3 [17]. The distributed high frequency model requires extra elements in addition to the conventional circuit, which are stator to frame capacitance($C_{sf}$), anti-resonance resistance ($\mu R_{sf}$), anti-resonance leakage inductance($\eta L_{ls}$), stator turn to turn capacitance($C_{sw}$), and stator turn to turn damping resistance($R_{sw}$). In general, these parameters are determined by measuring the frequency response from dif-

Fig. 4. Experimental setup for DM and CM test of a 5hp induction motor.

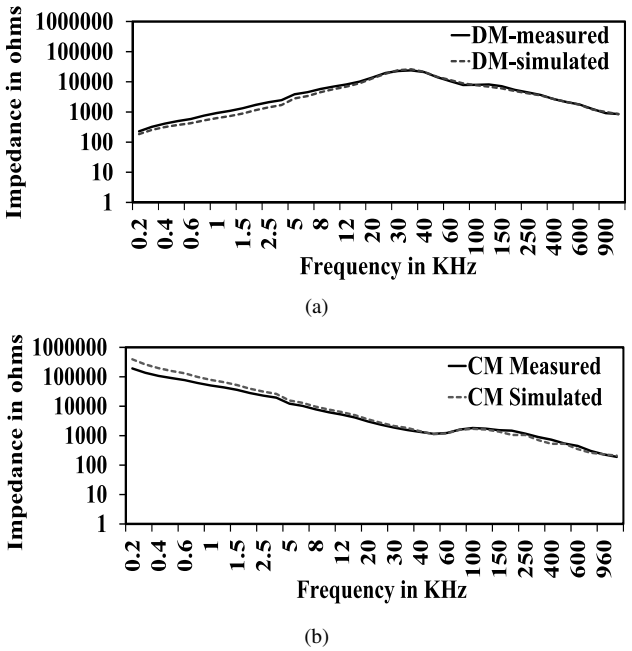


Fig. 5. 5hp induction motor measured and simulated frequency responses in DM and CM test

ferential mode test setup and common mode test setup. A three-phase, 5hp and 3hp 400/440V, 4pole Induction Motor with 36slots, 6coils per phase are considered for the present study. Differential mode test was performed by connecting LCR meter between phase A and tied leads of phase B and phase C. This test procedure is recommended for an ungrounded motor frame and LCR meter is put in Z-θ mode. Common mode test was performed with ground frame as one probe and phase A, phase B and phase C motor leads tied together to form the second probe to LCR meter in Z-θ mode. The experimental setup for differential mode test and common mode test is shown in Fig. 4. Figure 5 shows the impedance versus frequency responses measured with LCR meter and simulation for a 5hp motor under differential mode(DM) and common mode(CM). Similarly fig. 6 illustrates the impedance versus frequency in case of 3hp motor. The results demonstrated that the impedance versus frequency response observed in simulation closely matches with response measured on practical machine for DM and

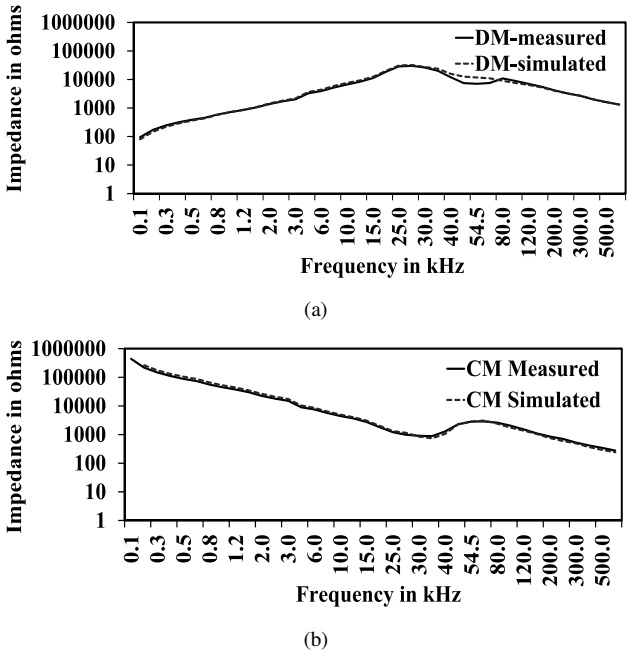


Fig. 6. 3hp induction motor measured and simulated frequency responses in DM and CM test

CM. Hence the considered model is valid for transient studies.

## 5. Verification of Algorithm with Simulation Data

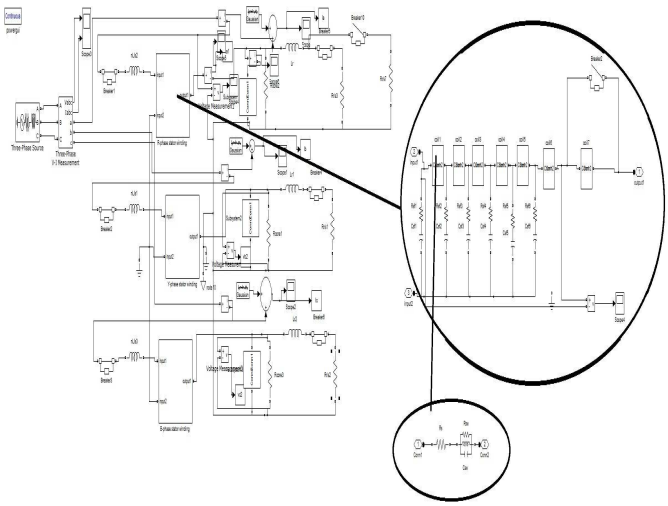

Fig. 7. Simulink model for stator inter-turn fault on a 3hp three-phase induction motor.

The simulation of stator inter-turn fault is built using distributed parameter model as mentioned in above section. The simulated motor is a three-phase, 3hp, 4pole, 415V, 50Hz squirrel cage induction motor with 36slots and 6coils per phase. Various percentages of turn level short circuits in different phases have been simulated in MATLAB/Simulink environment. Fig. 7 shows simulation model for stator inter-turn fault in R-phase with a short circuit level of 4-turns. A

short circuit between the turns in a stator phase causes an unbalance in stator currents. Fig. 8 shows the three- phase stator currents and three-phase residues under stator inter-turn fault in R-phase with a short circuit level of 4-turns. Figure 9(a) shows Fault indices along with adaptive threshold $Th1$. The variations in three-phase energy values along with adaptive threshold $Th2$ are illustrated in Fig. 9(b), where the maximum energy of faulty phase is higher than healthy phase. Thus, the proposed algorithm has successfully detected and identified the fault.

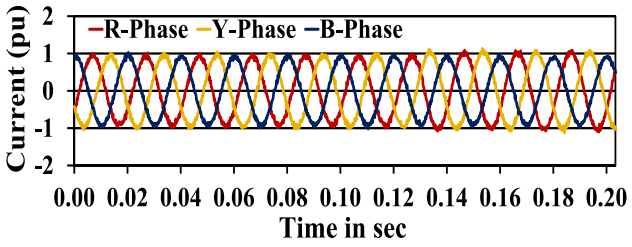


(a)

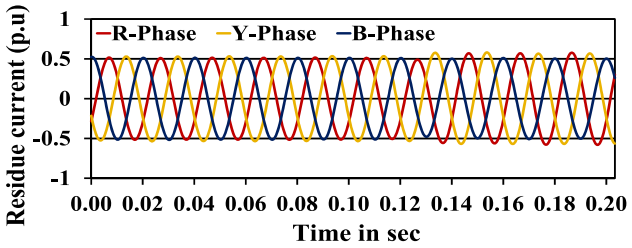


(b)

Fig. 8. Three-phase actual and residue currents for 4-turn short circuit in R-phase

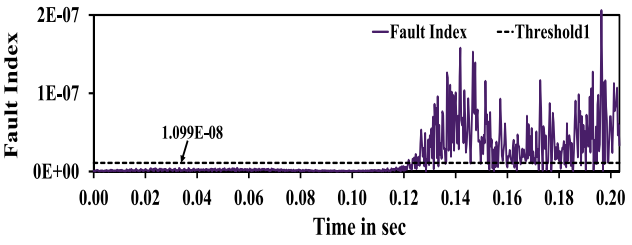


(a)

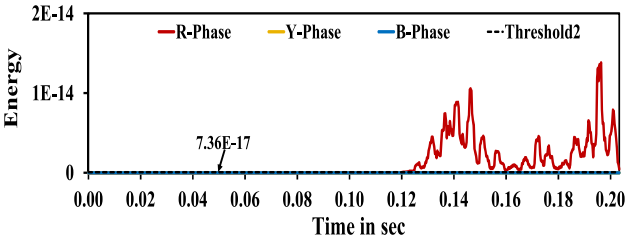


(b)

Fig. 9. (a) Fault indices for 4-turn short circuit in R-phase (b) Three-phase energies for 4-turn short circuit in R-phase.

## 6. Verification of Algorithm with Experimental Data

### 6.1 Experimental Setup

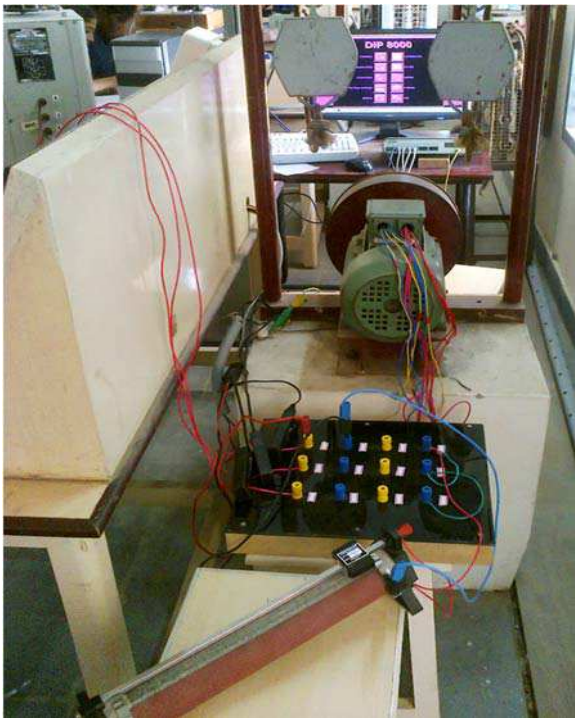

Fig. 10. Experimental setup for 3hp three-phase induction motor.

An experimental setup was prepared with a 3hp, 4-pole, 50Hz, and 415V three-phase induction motor with 36slots, 6coils per phase and 72 turns per coil. In order to create the inter-turn short circuit, two tapping points are taken out per phase from the neutral of the stator winding. The three-phase stator currents are captured with data acquisition system of network analyser (DIP8000). Figure 10 shows the experimental setup for stator inter-turn faults.

### 6.2 Experimental Results

Several current measurements are made by using power network analyser (DIP800) under various conditions such as healthy, stator inter-turn faults in different phases and sudden change in mechanical load. The three-phase currents are captured with a sampling frequency of 6.6 KHz and sent to PC through data acquisition card. Figure 11(a), (b) and (c) of left side show variations in three-phase stator currents under the above three conditions respectively. In practice, the raw signal is always corrupted with some noise. In addition to that the signal also has some harmonic components trigged by supply unbalance and machine unbalances. Hence, signal reconstruction should be required for stator inter-turn faults. The three-phase residue currents are obtained by preprocessing the captured three-phase currents with SWT of level based threshold.

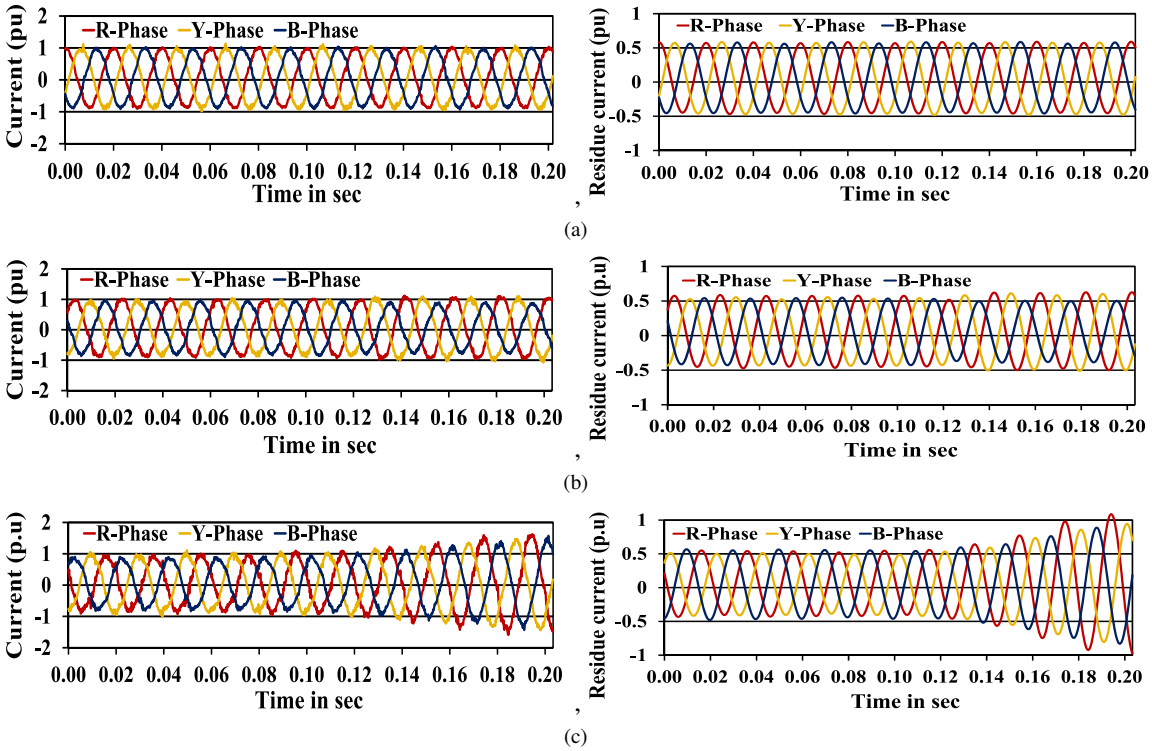


Fig. 11. Three-phase currents of actual (left) and residues (right) under three conditions: (a) healthy, (b) 4-turns shortened in R-Phase and (c) mechanical load change.

The variations in these residues for healthy, faulty and sudden change in mechanical load are shown in right side of Fig. 11(a), (b) and (c) respectively. The residue of three-phase stator currents are again decomposed with a DWT of Bior5.5 and calculated the slope of $d1$ coefficients to extract fault feature. The sum of absolute slope of the $d1$ coefficients are set as a fault index. The abnormal condition of the induction motor can be identified by checking the count value of three consecutive fault indices with respect to adaptive threshold $Th1$ and it should be greater than 6. Figure 12(a), (b) and (c) shows the variation in fault indices corresponding to healthy, stator inter-turn fault and sudden change in mechanical load respectively. Figure 13(a) and (b) show the energy variations due to stator inter-turn fault and sudden change in mechanical load respectively. The stator inter-turn fault can be identified by finding the difference between the $Loc1$ and $Loc2$ which are defined in section 3. If the difference between the two locations is within half cycle(10 ms), stator inter-turn fault is set to occur otherwise, the disturbance is due to sudden change in mechanical load. From experimental results it is observed that the difference in disturbance locations for stator inter-turn fault is 3 ms and for sudden change in mechanical load is 27 ms.

The faulty phase is identified by comparing the maximum value of energy in three-phases over a window size of one and half cycle from the fault instant. Figure 14 shows identification of faulty phase for stator inter-turn faults of R-Phase. The results show that the faulty phase energy is greater than the adaptive threshold $Th2$ and also higher than the healthy phases.

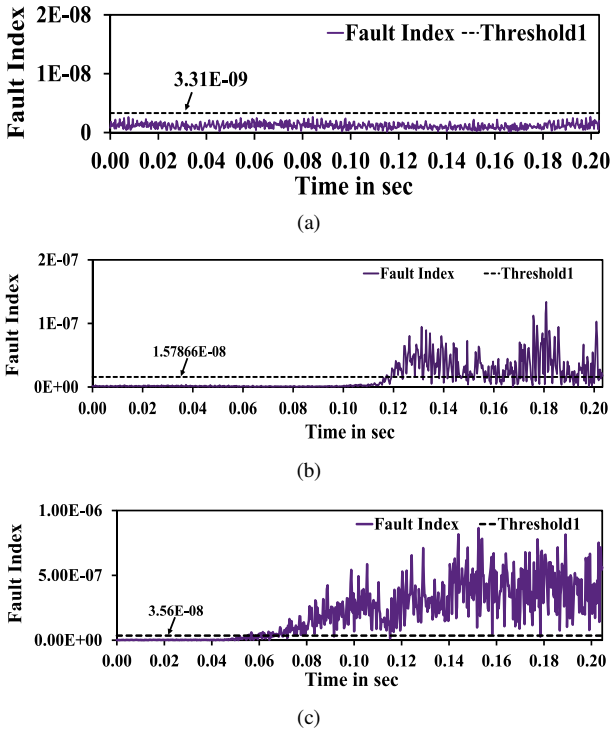


Fig. 12. Fault indices of a 3hp induction motor under three conditions: (a) Healthy (b) 4-turns short circuit in R-phase (c) Mechanical load change.

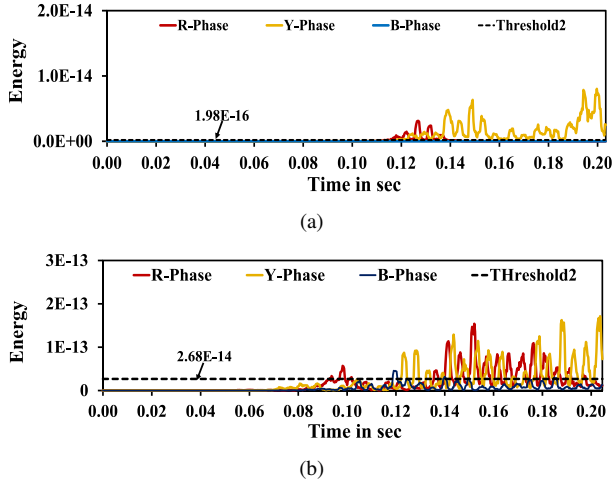


Fig. 13. Three-phase energies of a 3hp induction motor: (a) stator inter-turn fault in R-Phase (b) Mechanical load change.

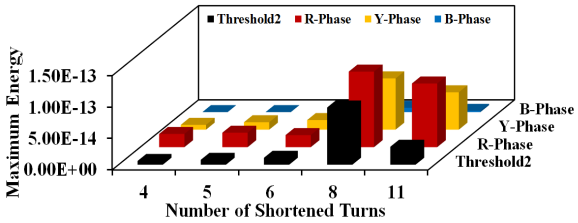


Fig. 14. Three-phase maximum energies for stator inter-turn faults in R-phase.

## 7. Comparison of Simulation results with Practical results

To verify the effectiveness of the proposed scheme, the same experimental induction motor is considered to simulate various levels of stator inter-turn faults in MATLAB/Simulink environment. The simulated cases and experimental cases are built with same conditions. Figure 15 shows the variation of maximum energy values for different levels of short circuited turns in R-phase of a stator winding under practical and simulation conditions. The results show that the maximum energy of the faulted phase is greater than the adaptive threshold $Th2$ and it is higher than healthy phases. The variations of maximum energy in 4-turns, 5-turns, 6-turns, 8-turns and 11-turns of simulation are nearly same as the practical. This establishes a good agreement between simulation and practical results.

The sensitivity index of the stator inter-turn fault is calculated based on the ratio of post-fault residue energy to pre-fault residue energy. Figure 16(a), (b) and (c) show that the sensitivity indices values for various levels of inter-turn shorted faults in R-phase, Y-phase and B-phase respectively. The results show that, the sensitivity index has increased with the increase in number of short-circuited turns. The estimated severity of different levels of stator winding short circuit under simulation is in good agreement with the practical one. The results obtained with real data deviated from those obtained with simulation data because of magnetic inductance and the presence of noise level in practical case.

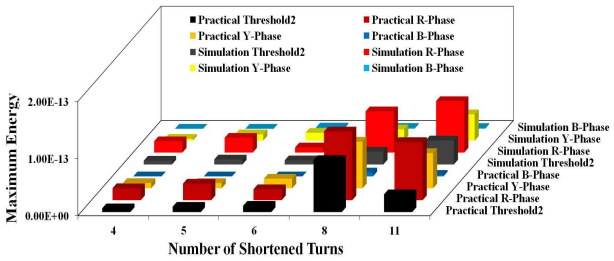


Fig. 15. Comparison of practical and simulated three-phase maximum energies for stator inter-turn fault in R-phase.

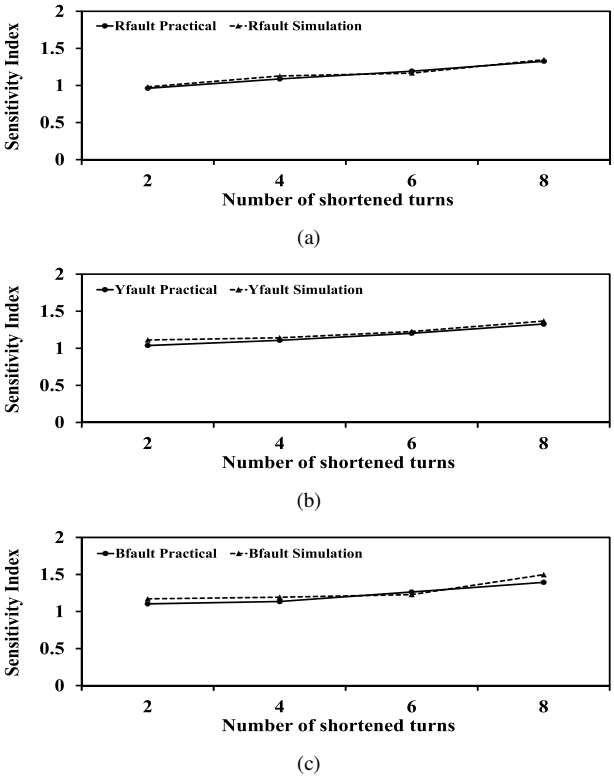


Fig. 16. Fault severity of a 3hp induction motor for stator inter-turn faults a) R-phase b) Y-phase c) B-phase.

## 8. Conclusions

This paper describes a Wavelet and adaptive threshold based fault diagnosis technique for a three-phase induction motor stator inter-turn faults. Fault residue currents are obtained from the inverse stationary wavelet transform of Bior5.5 mother wavelet. The use of SWT instead of DWT in reconstruction processes improve the denoising performance due to shift invariance property of SWT. The performance of proposed detection algorithm should improve the accuracy due to adaptive thresholds. The simulation and exper-

imental results demonstrate that the proposed algorithm is effective in detecting and identifying the faults. In addition to above, this paper also illustrates the severity of fault very effectively.

## References


[1] El Hachemi Benbouzid, M., 2000. "A review of induction motors signature analysis as a medium for faults detection". *IEEE Transactions on Industrial Electronics,* **47**(5), pp. 984–993.

[2] Group, I. M. R. W., 1985. "Report of large motor reliability survey of industrial commercial installations". *IEEE Transactions on Industry Applications Part II,* **IA**(21), pp. 853–872.

[3] Siddique, A., Yadava, G., and Singh, B., 2005. "A review of stator fault monitoring techniques of induction motors". *IEEE Transactions on Energy conversion,* **20**(1), pp. 106–114.

[4] Grubic, S., Aller, J. M., Lu, B., and Habetler, T. G., 2008. "A survey on testing and monitoring methods for stator insulation systems of low-voltage induction machines focusing on turn insulation problems". *IEEE Transactions on Industrial Electronics,* **55**(12), pp. 4127–4136.

[5] Zhang, P., Du, Y., Habetler, T. G., and Lu, B., 2011. "A survey of condition monitoring and protection methods for medium-voltage induction motors". *IEEE Transactions on Industry Applications,* **47**(1), pp. 34–46.

[6] Cruz, S. M., and Cardoso, A. M., 2001. "Stator winding fault diagnosis in three-phase synchronous and asynchronous motors, by the extended park's vector approach". *IEEE Transactions on Industry applications,* **37**(5), pp. 1227–1233.

[7] Da Silva, A. M., Povinelli, R. J., and Demerdash, N. A., 2008. "Induction machine broken bar and stator short-circuit fault diagnostics based on three-phase stator current envelopes". *IEEE Transactions on Industrial Electronics,* **55**(3), pp. 1310–1318.

[8] De Angelo, C. H., Bossio, G. R., Giaccone, S. J., Valla, M. I., Solsona, J. A., and García, G. O., 2009. "Online model-based stator-fault detection and identification in induction motors". *IEEE Transactions on Industrial Electronics,* **56**(11), pp. 4671–4680.

[9] Joksimovic, G. M., and Penman, J., 2000. "The detection of inter-turn short circuits in the stator windings of operating motors". *IEEE Transactions on Industrial Electronics,* **47**(5), pp. 1078–1084.

[10] Sharifi, R., and Ebrahimi, M., 2011. "Detection of stator winding faults in induction motors using three-phase current monitoring". *ISA transactions,* **50**(1), pp. 14–20.

[11] Khan, M., Radwan, T. S., and Rahman, M. A., 2007. "Real-time implementation of wavelet packet transform-based diagnosis and protection of three-phase induction motors". *IEEE Transactions on Energy Conversion,* **22**(3), pp. 647–655.

[12] Das, S., Purkait, P., Dey, D., and Chakravorti, S., 2011. "Monitoring of inter-turn insulation failure in induction motor using advanced signal and data processing tools". *IEEE Transactions on Dielectrics and Electrical Insulation,* **18**(5), pp. 1599–1608.

[13] Hernández, O., and Olvera, E., 2009. "Noise cancellation on ECG and heart rate signals using the undecimated wavelet transform". In International Conference on eHealth, Telemedicine, and Social Medicine, 2009. eTELEMED'09., IEEE, pp. 145–150.

[14] Akshay, N., Jonnabhotla, N. A. V., Sadam, N., and Yeddanapudi, N. D., 2010. "ECG noise removal and QRS complex detection using UWT". In International Conference on Electronics and Information Engineering (ICEIE), 2010, Vol. 2, IEEE, pp. V2–438.

[15] Yang, Y., Kamboh, A., and Andrew, J., 2010. "Adaptive threshold spike detection using stationary wavelet transform for neural recording implants". In Biomedical Circuits and Systems Conference (BioCAS), 2010 IEEE, IEEE, pp. 9–12.

[16] Donoho, D. L., and Johnstone, I. M., 1994. "Threshold selection for wavelet shrinkage of noisy data". In Engineering in Medicine and Biology Society, 1994. Engineering Advances: New Opportunities for Biomedical Engineers. Proceedings of the 16th Annual International Conference of the IEEE, IEEE, pp. A24–A25.

[17] Mirafzal, B., Skibinski, G., Tallam, R., Schlegel, D., and Lukaszewski, R., 2007. "Universal induction motor model with low-to-high frequency-response characteristics". *IEEE Transactions on Industry Applications,* **43**(5), pp. 1233–1246.